Accelerated Publications

Structural Constraints Imposed by a Non-Native Disulfide Cause Reversible Changes in Rhodopsin Photointermediate Kinetics†

James W. Lewis, Istvan Szundi, and David S. Kliger*

Department of Chemistry and Biochemistry, University of California, Santa Cruz, California 95064

Received March 20, 2000; Revised Manuscript Received May 18, 2000

ABSTRACT: Suspensions of bovine rhodopsin in 2% lauryl maltoside detergent were treated with Cu(phen)$_3^{2+}$ to form a disulfide bridge between cysteines 140 and 222 which occur naturally in the bovine rhodopsin sequence. Absorption difference spectra were collected after excitation with a pulse of 477 nm light on the time scale from 1 μs to 690 ms, and the results were analyzed using global exponential fitting. Only two exponentials could be fit to data from the Cu(phen)$_3^{2+}$-treated rhodopsin, while three exponentials were needed to fit data either from untreated rhodopsin or from Cu(phen)$_3^{2+}$-oxidized rhodopsin after further dithiothreitol reduction. Dithiothreitol treatment of rhodopsin which had not been previously oxidized with Cu(phen)$_3^{2+}$ had no effect on the observed kinetics. Since the 140−222 disulfide has previously been shown to block transducin activation, its effects on rhodopsin activation are of considerable interest. Cu(phen)$_3^{2+}$ treatment favors formation of the meta I_{380} intermediate relative to meta I_{480} and slows formation of meta II from meta I_{380}. This suggests that the protein change involved in meta I_{380} formation is similar to the structural constraint introduced by the 140−222 disulfide. These results show that formation of disulfides in rhodopsin has potential as a tool for discriminating between the three isochromic, 380 nm absorbing intermediates involved in rhodopsin activation and for gaining insight into how their structures differ.

Studies of the mechanisms underlying the functions of rhodopsin and bacteriorhodopsin (BR)[1] have taken on added importance in recent years since hundreds of related heptahelical G-protein-coupled receptors have been identified, and more members of this family are likely to be found as a result of the human genome project. While analogies within the family have been useful in developing general structural ideas, so far only BR has produced crystals suitable for X-ray analysis (*1*). However, results from BR crystals are not directly applicable to the receptor members of the heptahelical family since receptors differ significantly in function from BR and also show a different arrangement of helices in cryoelectron microscopy (*2*). Even if X-ray structural data were available for a heptahelical receptor, it is by no means certain to reveal the mechanism of activation. This is particularly so given that the rhodopsin photointermediates which can be trapped at low temperatures, and hence which are suitable for X-ray study, are known to differ from those which occur at physiological temperatures (*3*). It is thus of great interest to directly gain structural information about the physiological intermediates using time-resolved techniques.

Disulfide bonds provide an infallible marker of side chain proximity in proteins where they occur. Proximity can be determined either from the occurrence of native disulfides or from cysteines introduced through genetic modification techniques which can be scanned through the sequence positions of a split version of the protein of interest. This latter technique has been used recently to map out tertiary interactions in the rod cell visual pigment, rhodopsin (*4*). Despite the importance of disulfides as markers of structure, that role is necessarily secondary to their function as constraints on structure in proteins where they occur naturally. When a non-native disulfide is introduced into a protein like rhodopsin, which is susceptible to time-resolved studies, any changes which are observed in specific kinetic steps can be associated with the localized structural perturbation. A good deal is already known about the photointermediates of rhodopsin which appear after the initial chromophore isomerization and prior to activation of the G-protein, transducin. To develop a better structural picture of these intermediates and hence of the mechanism of heptahelical receptor protein activation, it would be useful to associate specific spatial constraints with time scales of action. Two such non-native disulfides have separately been shown to reversibly inhibit transducin activation while leaving the pigment spectrum unaffected (*5*), an observation which constitutes measurement of an effect at essentially the lowest level of time resolution. Our goal in the work presented here was to study at higher time resolution the effect of an inactivating, non-native disulfide on rhodopsin and to relate the observed kinetic changes seen in time-resolved absorption

† This work was supported by Grant EY00983 (to D.S.K.) from the National Eye Institute of the National Institutes of Health.

[1] Abbreviations: BR, bacteriorhodopsin; DTT, dithiothreitol; lumi, lumirhodopsin; meta, metarhodopsin; PBS, phosphate-buffered saline.

10.1021/bi0006363 CCC: $19.00
Published on Web 06/16/2000

spectra to specific reaction steps in the photoactivating sequence.

An unexpected consequence of the cysteine scanning split receptor, tertiary mapping work was the observation that treatment with $Cu(phen)_3^{2+}$ induced disulfide formation between Cys140 and Cys222 in the native bovine rhodopsin sequence, in both the full-length and split versions of the rhodopsin receptor. A model based on electron diffraction data places Cys140 at the cytoplasmic end of helix III, oriented toward the face of helix V containing Cys222, but places Cys222 approximately two helix turns deeper in the membrane than Cys140 (*6*). Formation of the 140−222 disulfide is expected to affect the bleaching kinetics since removal of the single native rhodopsin disulfide in the C110A/C187A mutant has been reported to affect the stability of the metarhodopsin (meta) II intermediate (*7*), even though that mutant continued to exhibit normal initial rates of transducin activation. Here we report significant changes in absorption kinetics under conditions in which the 140−222 disulfide is formed and the quantitative reversal of those changes by treatment with dithiothreitol (DTT).

MATERIALS AND METHODS

Preparation of Rhodopsin Samples. Rod outer segments were prepared as described previously (*3*) from frozen bovine retinas (J. A. Lawson, Omaha, NE). Extrinsic membrane proteins were removed by hypotonic washing with pH 7.0, 1 mM EDTA solution, and the final pellet after centrifugation was resuspended in 2% lauryl maltoside detergent in PBS [20 mM $NaHPO_4$, 60 mM KCl, 30 mM NaCl, 2 mM $MgCl_2$, and 0.1 mM EDTA (pH 7.0)] so that the final rhodopsin concentration was 2 mg/mL. For samples treated with $Cu(phen)_3^{2+}$, 9 mM phenanthroline, 3 mM $CuSO_4$, and 2% glycerol were added to the detergent suspension as described by Yu and Oprian (*5*). Immediately after addition, these samples were incubated for either 30 or 60 min at 37 °C in a water bath. Following incubation, samples were passed through a G-50 column to remove $Cu(phen)_3^{2+}$, and half the sample eluted from the column was used immediately for photochemical kinetic measurements. The other half of the eluted sample was incubated overnight (24 h) at room temperature after addition of 25 mM DTT. Immediately prior to optical measurements, any sedimentable material was removed by centrifugation and samples were degassed at room temperature by gently agitating them under vacuum.

Collection of Time-Resolved Absorbance Difference Spectra. Individual 1 μL samples were photolyzed at 20 °C by 7 ns (fwhm) laser pulses. A dye laser, pumped by the 355 nm third harmonic of a Nd:YAG laser, was used to produce vertically polarized 477 nm light. The energy flux delivered to the sample was 80 $\mu J/mm^2$. The change in absorption spectrum at a particular time delay, ranging from 1 μs to 690 ms after photolysis, was measured using a gated optical multichannel analyzer (*8*). Absorbance changes were monitored perpendicularly to the excitation beam using a flashlamp to produce white light that was polarized at 54.7° relative to the laser polarization direction. The path lengths of the actinic light and probe light in the sample were 0.5 and 2 mm, respectively.

Data Analysis. The set of experimental difference spectra, $\{\Delta A(\lambda,t)\}$, were fit as described previously (*9*) to a function whose form was a sum of exponential decays:

$$\Delta a(\lambda,t) \equiv b_0(\lambda) + b_1(\lambda)\exp(-t/\tau_1) + b_2(\lambda)\exp(-t/\tau_2) + \ldots$$

The apparent lifetimes, τ_i, and the difference spectra associated with the individual lifetimes or *b* spectra, $b_i(\lambda)$, are unambiguously determined by the fitting process, but exponential fitting does not determine a unique chemical scheme or mechanism. Data for detergent suspensions of rhodopsin on the time scale after photolysis studied here have been shown to be best described by a square scheme (*10*):

$$\begin{array}{ccc} \ldots \text{ lumi} & \underset{k_2}{\overset{k_1}{\rightleftharpoons}} & \text{meta } I_{380} \\ k_3 \downarrow & & \downarrow k_4 \\ \text{meta } I_{480} & \underset{k_6}{\overset{k_5}{\rightleftharpoons}} & \text{meta II} \ldots \end{array}$$

where lumirhodopsin (lumi) is fully formed within 1 μs, which is the time at which our first absorbance difference spectrum is collected here. The product of lumi decay is either the traditional metarhodopsin I (meta I_{480}) or meta I_{380}, an intermediate which begins to appear above 20 °C in membrane suspensions of rhodopsin and whose formation is favored by the presence of detergent. The microscopic rate constants, k_i, appropriate for this mechanism under each set of sample conditions were determined by fitting the *b* spectra obtained from each experiment using intermediate spectra as described previously (*11*).

RESULTS

Figure 1 compares absorbance difference spectra collected after photolysis of the $Cu(phen)_3^{2+}$-treated rhodopsin sample to difference spectra collected from a similar untreated sample and to spectra collected from an aliquot of the $Cu(phen)_3^{2+}$ sample after DTT reduction. The data show that $Cu(phen)_3^{2+}$ treatment speeds formation of a 380 nm absorbing product and that the effect is completely reversed by DTT treatment. The $Cu(phen)_3^{2+}$ treatment has no effect on the earliest and latest difference spectra, which are unchanged within the noise level for all three samples (after scaling). $Cu(phen)_3^{2+}$ incubation for 60 min was more than sufficient to produce the full effect as shown by the fact that data collected after incubation for 30 min were essentially identical to those presented in the middle panel of Figure 1. DTT treatment by itself had no effect on rhodopsin photobleaching kinetics in these detergent suspensions of rhodopsin (data not shown).

The data for the untreated rhodopsin were best fit by three exponential decays, as has been seen previously for purified rhodopsin samples at 20 °C (*10*). Similarly, three exponentials were required to fit the data for the $Cu(phen)_3^{2+}$ sample after DTT reduction. However, the $Cu(phen)_3^{2+}$-treated sample itself could only be fit with two exponentials, and the plot of residuals between the two-exponential fit and data for that sample was as flat as the residual plots for the other two samples when they were fit with three exponentials. The lifetimes (base e) for the fits are given in Table 1, and the *b* spectra associated with these lifetimes are shown in Figure 2. The amplitude of the components shown in Figure 2 must be kept in mind when comparing the lifetimes shown in

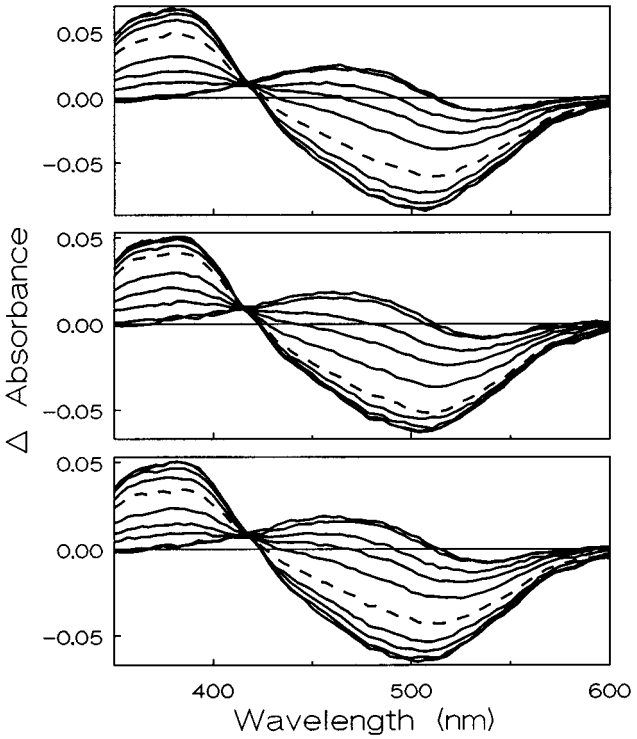

FIGURE 1: Absorption difference spectra collected after photolysis of rhodopsin solubilized in 2% lauryl maltoside. (Top) Untreated sample data collected at delays of 1, 10, 50, 100, 200, and 500 μs (- - -) and 1, 2, 10, and 690 ms relative to the 477 nm excitation pulse. (Middle) Data from the sample treated for 60 min with Cu(phen)$_3^{2+}$ collected at the same delay times. (Bottom) Cu(phen)$_3^{2+}$-treated sample after incubation for a further 24 h with 25 mM DTT. Absorption difference spectra were collected at the same delay times. The untreated sample used to collect the data shown here was diluted 3:7 with 2% lauryl maltoside in PBS to compensate for dilution of the Cu(phen)$_3^{2+}$-treated sample after passage through the G-50 column.

Table 1: Lifetimes of Decay Components Observed on the Microsecond Time Scale after Photolysis

sample conditions	τ_1 (μs)	τ_2 (μs)	τ_3 (ms)
rhodopsin (2% lauryl maltoside in PBS)	120	460	2.4
Cu(phen)$_3^{2+}$-treated rhodopsin	150	1000	*a*
DTT-reduced, Cu(phen)$_3^{2+}$-treated rhodopsin	100	500	6.4

[a] No slow component was observed in this sample.

Table 1 since the lifetimes of the smaller components are necessarily less well determined than are the lifetimes associated with the larger amplitude *b* spectra. The kinetics of the untreated and DTT-reduced samples exhibited three apparent lifetimes and are satisfactorily described by the square model originally derived for membrane-bound rhodopsin. The kinetics of the Cu(phen)$_3^{2+}$-treated sample show two apparent lifetimes, and the corresponding *b* spectra show the decay of lumi in two steps, both producing 380 nm absorbing products. This implies that lumi is connected to the next intermediate, a 380 nm absorber, via a significantly reversible step since if the first decay of lumi were unidirectional, a single apparent lifetime would result for lumi decay (i.e., the second process would not result in an observable spectral change as the two intermediates involved in that process are isospectral). The second process detected here indicates a final product forming which is also a 380 nm absorber and which must be produced by an essentially irreversible reaction. The amplitude of lumi absorbance found in the two

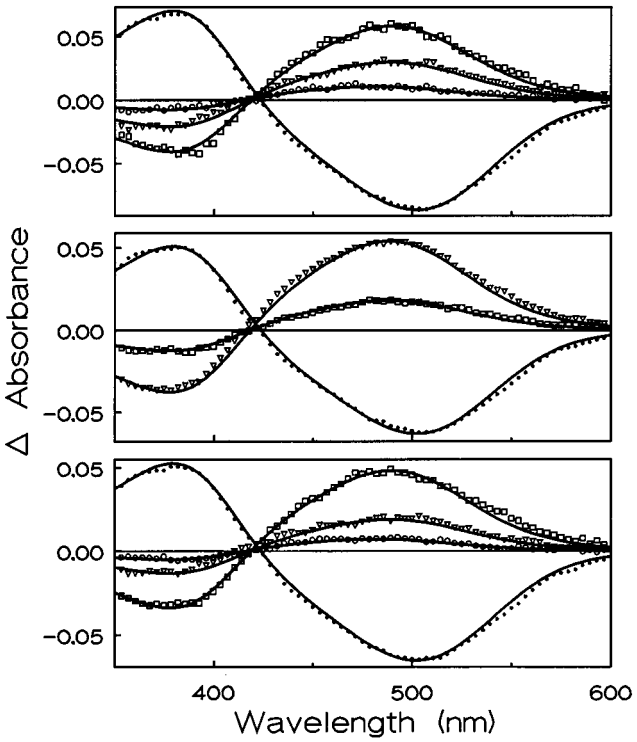

FIGURE 2: Comparison of *b* spectra from exponential fitting with those determined from the square mechanism. Symbols show *b* spectra determined from fitting the data depicted in Figure 1 (▽, τ_1; □, τ_2; ○, τ_3; ●, b_0). Smooth lines show the *b* spectra calculated from the square mechanism using the rate constants given in Table 2.

Table 2: Microscopic Rate Constants Determined from Fitting the Square Mechanism to Absorption Difference Spectra

	rhodopsin	Cu(phen)$_3^{2+}$	Cu(phen)$_3^{2+}$ + DTT
k_1 (s^{-1})	3910	5140	3900
k_2 (s^{-1})	2230	1120	3220
k_3 (s^{-1})	260	0	230
k_4 (s^{-1})	4310	1250	4740
k_5 (s^{-1})	420	0	160
k_6 (s^{-1})	0	0	0

experimental *b* spectra from the Cu(phen)$_3^{2+}$-treated sample is consistent with such an interpretation. This scheme for the Cu(phen)$_3^{2+}$-treated sample is identical to the lumi $\rightleftharpoons$ meta I_{380} $\rightarrow$ meta II sequence in the square model.

The microscopic rate constants obtained by fitting the data to the square model are given in Table 2. Agreement of the fit (line) with the data (symbols) can be seen in Figure 2. As is usually the case for detergent suspensions of rhodopsin, no observable back reaction from meta II to meta I_{480} was detected. Determination of the microscopic rates allows the concentration of the intermediate species to be calculated. The temporal profiles of the photointermediate concentrations determined from the fit are shown in Figure 3.

DISCUSSION

We see significant kinetic changes under the conditions which produce a Cys140−Cys222 disulfide in rhodopsin, and the original kinetic behavior is quantitatively recoverable by treatment with the disulfide reducing agent DTT. This conclusion is apparent from inspection of the raw data presented in Figure 1 and is further supported by the results

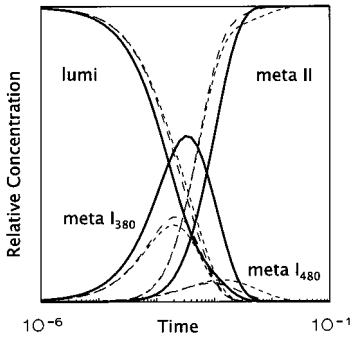

FIGURE 3: Temporal profile of photointermediate concentrations determined from the square model. Decay of lumirhodopsin is accompanied by the rise of meta I_{380} which is in turn followed by the growth of meta II at long times. For the untreated sample and the DTT-treated, $Cu(phen)_3^{2+}$-oxidized sample, a small amount of meta I_{480} builds up in parallel with the decay of meta I_{380} to meta II, but no meta I_{480} forms in the $Cu(phen)_3^{2+}$-oxidized sample unless it is reduced with DTT. Solid lines show photointermediates for the $Cu(phen)_3^{2+}$-oxidized sample, and dashed lines show intermediates for rhodopsin (− − −) and for the DTT-treated, $Cu(phen)_3^{2+}$-oxidized sample (- - -).

of global exponential fitting. The *b* spectra in the lower panel of Figure 2 show that the changes seen in the middle panel of that figure, produced by $Cu(phen)_3^{2+}$ oxidation, are completely reversed by DTT. Analysis of these *b* spectra in terms of the square mechanism intermediates shows that formation of the 140−222 disulfide favors the meta I_{380} side of the square scheme by shifting forward the equilibrium between lumi and meta I_{380}. The rates in Table 2 show that this is accomplished both by accelerating meta I_{380} formation and by retarding the reverse reaction. The fact that the 1 μs difference spectrum for the $Cu(phen)_3^{2+}$-treated sample exhibits a normal lumi − rhodopsin difference spectrum suggests that events up to lumi are unperturbed by formation of the 140−222 disulfide. Therefore, the changes seen in k_1 and k_2 show that beginning with the barrier between lumi and meta I_{380}, 140−222 disulfide formation starts to affect the reaction pathway followed, presumably by stabilizing meta I_{380}. Meta I_{380} stabilization is also consistent with the slowing of its decay to meta II seen in the reduced value of k_4. Since the 140−222 disulfide is some distance from the chromophore pocket, it is reasonable that the earliest intermediates are unaffected, as those intermediates involve changes localized to the pocket.

The introduction of a non-native disulfide could have perturbed rhodopsin sufficiently that the square scheme was fundamentally inapplicable, as, for example, by eliminating the back reaction from meta I_{380} to lumi. However, while oxidation confines the square scheme to the right-hand branch from lumi, our data clearly show that a significant back reaction from meta I_{380} to lumi remains. The fact that we see two time constants for decay of lumi absorbance *requires*, as discussed above, an initial decay into equilibrium with a 380 nm absorbing species. Further, the continued applicability of the basic features of the square scheme to the $Cu(phen)_3^{2+}$-treated sample is shown by the absence of any back reaction between meta II and meta I_{380} in that sample. If any such back reaction were introduced by oxidation, incomplete decay of lumi absorbance would take place, and this is not observed. For detailed analysis of these alternative schemes and the reason for their inapplicability here, see ref 11.

A model of rhodopsin structure based on cryoelectron microscopy results (*6*) places Cys140 very near the cytoplasmic end of helix III, the rhodopsin helix most tilted away from the membrane normal. The rotational orientation of helix III is fairly well determined because it contains the chromophore Schiff base counterion, Glu113, which must point toward the chromophore. This orientation points Cys140 roughly in the direction of helix V, which contains Cys222. The rotational orientation of helix V is less well determined than helix III; however, the helix does contain His211 which is known to interact with the chromophore (*12*), and the orientation of His211 toward the chromophore orients Cys222 toward helix III. These arguments show that 140−222 disulfide formation is consistent with what is known about the orientation of these groups in the plane of the membrane. However, the α-carbon coordinates of the Baldwin model place Cys222 roughly two helix turns deeper in the membrane than Cys140. Since both of these helices have odd numbers, the side chain orientation for both cysteines is downward into the membrane, so this factor does not relieve the mismatch. Consequently, it seems likely that the disulfide does not form at the equilibrium spacing of these two cysteines but forms at some nonequilibrium position created by thermal fluctuations. This character is consistent with $Cu(phen)_3^{2+}$ being required to form the disulfide bond (oxygen alone is not sufficient; *5*) and the fact that the 140−222 disulfide can be reduced by DTT. The fact that the 140−222 disulfide is relatively strained is further supported by the observation that when a cysteine is engineered into rhodopsin about one turn above position 222, at position 225 in helix V, a 140−225 disulfide forms spontaneously without $Cu(phen)_3^{2+}$ and the 140−225 disulfide does not prevent transducin activation (*5*). Comparison of the effects of other introduced cysteines on transducin activation is useful for determining whether the 140−222 disulfide acts to constrain helix translation or rotation. In this context, it should be noted that a disulfide between a cysteine introduced at position 136 and the native cysteine at position 222 also makes rhodopsin inactive toward transducin (*5*). Movement of the cysteine from position 140 to 136 should rotate the disulfide by 40° around helix III, making disulfide action through a similar rotational constraint in both the 140−222 and 136−222 cases unlikely. This leaves open the possibility that an essentially translational separation of helices III and V is involved in activation, and that this translation is inhibited by either disulfide. From our current results, it appears that an opposite motion is involved in meta I_{380} formation, but this conclusion must be considered tentative until further kinetic studies can be conducted on the mutant pigments discussed above.

Previously, three separate disulfides engineered into rhodopsin which cross-linked helices III and VI (139−248, 139−250, and 135−250) were shown to inhibit transducin activation (*13*). Those observations were interpreted in terms of transducin activation requiring relative motion between helices III and VI. Such motion is not inconsistent with relative motion of helix III relative to helix V which we observe here, and the fact that we see meta II formation in the absence of transducin activation is also consistent with what was seen there in the case of the helix III−helix VI cross-links.

In terms of the receptor activation mechanism, our results reinforce the picture that Schiff base deprotonation alone does not constitute activation. It is tempting to propose that the thermal fluctuation trapped by disulfide 140−222 formation represents the extremum of a protein conformational breathing motion which normally acts in concert with a deprotonated Schiff base to cause proton uptake by meta II and transducin activation. It is reasonable to assume that such conformational motion could be affected by disulfide formation, and in fact, the native 110−187 disulfide has been shown to affect meta II stability (*7*).

It is not surprising that formation of the 140−222 disulfide prevents rhodopsin activation since conformational changes in the loop at the end of helix III, beginning near Cys140, are known to be involved in the interaction with transducin (*14*). In terms of what is known concerning the photointermediates involved in activation, the 140−222 disulfide presumably blocks proton uptake by meta II, preventing formation of the transducin activating form, meta II_b (*15*). This, too, is not surprising since Glu134, the residue which has been associated with this proton uptake (*16*), is also very close to position 140. Given that all intermediates known to precede meta II_b make their appearance in the $Cu(phen)_3^{2+}$-treated samples, it must be this final proton uptake which is inhibited by the formation of the 140−222 disulfide. Direct observation of the absence of proton uptake is theoretically possible using the pH indicator dye bromcresol purple, but in practice at high detergent concentrations, as is the case for the samples studied here, too much buffering exists to conduct the proton uptake measurements.

The results we present here show that the non-native, 140−222 disulfide has promise for discriminating among the three isochromic, 380 nm absorbing intermediates which appear late in the activation sequence. By stabilizing the unprotonated form of meta II, it also opens up these intermediates to study using other techniques. Previously, using FTIR measurements, Cys222 was proposed as a possible site undergoing environmental change in meta II formation (*17*), and the 140−222 disulfide preparation could be useful in extending those studies. Given the importance of understanding the activation mechanism of heptahelical receptor proteins, it is important that the fortunate discovery of the 140−222 disulfide be promptly exploited, employing the broadest range of techniques possible.

REFERENCES

1. Luecke, H., Schobert, B., Richter, H. T., Cartailler, J. P., and Lanyi, J. K. (1999) *Science 286*, 255−260.
2. Unger, V. M., Hargrave, P. A., Baldwin, J. M., and Schertler, G. F. X. (1997) *Nature 389*, 203−206.
3. Thorgeirsson, T. E., Lewis, J. W., Wallace-Williams, S. E., and Kliger, D. S. (1993) *Biochemistry 32*, 13861−13872.
4. Struthers, M., Yu, H., Kono, M., and Oprian, D. D. (1999) *Biochemistry 38*, 6597−6603.
5. Yu, H., and Oprian, D. D. (1999) *Biochemistry 38*, 12033−12040.
6. Baldwin, J. M., Schertler, G. F. X., and Unger, V. M. (1997) *J. Mol. Biol. 272*, 144−164.
7. Davidson, F. F., Loewen, P. C., and Khorana, H. G. (1994) *Proc. Natl. Acad. Sci. U.S.A. 91*, 4029−4033.
8. Lewis, J. W., and Kliger, D. S. (1993) *Rev. Sci. Instrum. 64*, 2828−2833.
9. Hug, S. J., Lewis, J. W., Einterz, C. M., Thorgeirsson, T. E., and Kliger, D. S. (1990) *Biochemistry 29*, 1475−1485.
10. Szundi, I., Mah, T. L., Lewis, J. W., Jäger, S., Ernst, O. P., Hofmann, K. P., and Kliger, D. S. (1998) *Biochemistry 37*, 14237−14244.
11. Szundi, I., Lewis, J. W., and Kliger, D. S. (1997) *Biophys. J. 73*, 688−702.
12. Weitz, C. J., and Nathans, J. (1993) *Neuron 8*, 465−472.
13. Cai, K., Klein-Seetharaman, J., Hwa, J., Hubbell, W. L., and Khorana, H. G. (1999) *Biochemistry 38*, 12893−12898.
14. Konig, B., Arendt, A., Mcdowell, J. H., Kahlert, M., Hargrave, P. A., and Hofmann, K. P. (1989) *Proc. Natl. Acad. Sci. U.S.A. 86*, 6878−6882.
15. Hofmann, K. P., Jäger, S., and Ernst, O. P. (1995) *Isr. J. Chem. 35*, 339−355.
16. Arnis, S., Fahmy, K., Hofmann, K. P., and Sakmar, T. P. (1993) *J. Biol. Chem. 269*, 23879−23881.
17. Rath, P., Bovee-Geurts, P. H. M., DeGrip, W. J., and Rothschild, K. J. (1994) *Biophys. J. 66*, 2085−2091.

BI0006363